

# MEMS Deformable Mirror for Ophthalmic Imaging

Yuhua Zhang, Austin Roorda

School of Optometry, University of California, Berkeley, Berkeley, CA, USA 94720-2020

## ABSTRACT

A MEMS deformable mirror has recently been employed in the AO system of an adaptive optics scanning laser ophthalmoscope (AOSLO). MEMS allows for a more compact, efficient and effective system. The AO system in the AOSLO operates with a modal closed loop. Aberrations after AO reduce the wave aberration to less than 0.1 microns RMS in most eyes. Results show improved resolution, brightness and contrast. Images of patches of retina show a well resolved cone photoreceptor mosaic as they change in size with eccentricities ranging from 0.6 degrees to 4.23 degrees from the fovea.

**Keywords:** Adaptive optics, MEMS, ophthalmoscopy, scanning laser ophthalmoscope

## 1. INTRODUCTION

By correcting for the aberrations that cause blur in the retinal image, adaptive optics technology has allowed for direct viewing<sup>1</sup> and measurement of the properties of microscopic structure in the living human eye<sup>2-7</sup>. AO imaging offers the opportunity for investigations of structures and processes in the eye that previously were possible only in excised retinas from donor eyes, or in animal models. Real-time microscopic imaging in the adaptive optics scanning laser ophthalmoscope, or AOSLO<sup>8</sup>, permits direct visualization of dynamic activity such as microscopic eye movements<sup>9</sup> and flow of single leukocytes in the smallest retinal capillaries<sup>10</sup>.

Despite the effectiveness of adaptive optics for correcting the human eye, wide-spread and commercial use of AO technology in vision science has been limited because of the lack of effective and economical wavefront correctors. The standard technology has remained the *discrete-actuator-based* deformable mirrors, which are comprised of a continuous mirror face sheet fixed to an array of individually addressable actuators. The actuators are usually made from a piezoelectric material. From this point we will refer to them as discrete actuator deformable mirrors. These mirrors, such as the DMs made by Xinetics Inc. (Devens, MA), perform very well but the costs are prohibitive (about \$1500/actuator), the size is too large, and the stroke is limited to about 4 microns.

In the near decade since the first demonstration of effective AO retinal imaging<sup>1</sup>, several alternate correcting technologies have been tested but none have matched the ability of the discrete actuator deformable mirror. For example, inexpensive membrane mirrors<sup>11;12</sup> and bimorph mirrors<sup>13;14</sup> have large stroke but are limited in their ability to correct sufficiently high-order aberrations for the eye. Segmented transmissive LCD phase modulators have too few elements to work effectively for high order aberration correction<sup>15;16</sup>. Optically addressed LCD-based wavefront correctors require phase wrapping to achieve a high enough effective stroke and are thus limited to single wavelength imaging<sup>17-19</sup>. Furthermore, LCD wavefront correctors require polarized light which is problematic for the eye whose cornea and retina are known to alter and depolarize the light from the eye<sup>20;21</sup>.

Micro-electro-mechanical systems (MEMS) are the alternate technology that holds the greatest promise to deliver a deformable mirror that meets the specifications required for ophthalmic applications. The needs are well laid out by Doble and Miller<sup>22</sup> who carefully compute requirements based on two extensive population studies<sup>23;24</sup>. To summarize, correcting the high order aberrations of 95% of typical eyes over a 6 mm pupil using a continuous face-sheet deformable mirror with a small amount of cross talk between actuators requires about 100 actuators over the pupil and about 3-6 microns of stroke (correcting high orders only). It is also important that mirror be able to operate at frequencies above 30 Hz because of dynamic changes in aberrations in the eye<sup>25</sup>. In order to expand the correction to include moderate amounts of defocus and astigmatism in the population, the mirrors should ideally have about 10 microns of stroke or more. Although there are no MEMS mirrors that meet these requirements to date, the field has been developing rapidly and such mirrors are expected to be available before 2007.

The first use of MEMS for ophthalmic applications was reported by Doble et al who used an early MEMS DM from Boston Micromachines Corporation (Watertown, MA) in a flood-illuminated AO retinal camera<sup>26</sup>. The limited stroke of that early device (2 microns) limited their correction to a 4 mm pupil but, over that pupil size, the wavefront was flattened to a level equivalent that obtained with a 37 channel discrete actuator deformable mirror from Xinetics Inc.

Presently, MEMS mirrors are available with specifications that are comparable with the discrete actuator DMs and they are being tested in several laboratories. In this paper we present our initial results from an AOSLO equipped with a MEMS deformable mirror.

## 2. METHODS

### 2.1. Scanning Laser Ophthalmoscopy

A scanning laser ophthalmoscope (SLO) operates on identical principles to the scanning laser microscope<sup>27-29</sup>. An image is built over time by recording the scattered light from a focused spot as it scans in a raster pattern across the sample. By the law of reversibility the scattered light from the sample follows the reverse direction of the ingoing path and hence is 'descanned', which means that once the returning light reflects off the scanning mirrors, the beam is rendered stationary again. The descanning allows one to place a fixed aperture, called the confocal pinhole, in a retinal-conjugate position in the return path prior to the detector. The role of the confocal pinhole is to limit the light reaching the detector to that coming from the plane of focus, thereby providing high contrast images as well as conferring the ability to do optical sectioning of thick, weakly scattering tissue<sup>30</sup>.

The only difference between a scanning laser microscope and an SLO is that in an SLO the objective lens is always the optics of the eye and the sample is always the fundus of the eye. These differences do not fundamentally change the operation of the instrument, but they impose serious constraints on imaging performance. First, the numerical aperture (NA) is dictated by the available physiological pupil sizes that the eye can offer. With dilating agents, pupil sizes in the human eye peaks at about 8 mm, which converts to a maximum possible NA of 0.23. Practically, we are limited to about a 6 mm pupil, which has an NA of 0.18. The main constraint, however, is that at such large pupil sizes in the human eye, the aberrations of the cornea and lens severely degrade the image<sup>31</sup> so the benefits of the maximum NA are not realized. The role of adaptive optics in an SLO (or any ophthalmoscope) is to correct the ocular aberrations over these large pupils and obtain the best possible images of the eye's fundus.

### 2.2. Specific AOSLO Details

The optical layout of the AOSLO is shown in figure 1. The optical path is comprised of a series of telescopes which relay the light from one pupil conjugate to the next. The relationships between the pupil conjugate positions in the imaging system are as follows: A 6 mm pupil at the eye projects to 3 mm at the slow scan mirror, 2 mm at the fast scan mirror, 4 mm at the DM and 5.33 mm at the lenslet array of the Shack Hartman wavefront sensor as well as at the collector lens for the confocal pinhole and detector. Because we reflect off the DM at a rather steep angle of incidence (24 degree optical deflection angle) the pupil actually projects as an ellipse onto the DM. Figure 2 shows the relative geometry of the pupil, the wavefront sensor lenslets and the DM actuator locations. The Shack Hartman wavefront sensor has a 328-micron pitch and 24-mm focal length lenslets. As such, the wavefront over a 6 mm pupil in the eye is sampled at 213 locations.

The AOSLO uses an 840 nm broadband low-coherence light source (Broadlighter S840-HP, Superlum, Russia), output from a single mode fiber at the source. The low-coherent source is used to reduce interference artifacts and speckle in the images<sup>32</sup>. A frame is constructed by combining the scan mirror location information, in the form of an *hsync* and a *vsync* signal, with the detected light information, which is measured with a photomultiplier tube (Hamamatsu, Japan). The frame grabber digitizes pixels at a 20 Mhz detection rate to generate 8-bit 512 X 512 frames at 30 frames per second. The extent of the scanned field can be adjusted continuously from 0.75 X 0.75 to 4 X 4 degrees

in angular extent (approximately 225 X 225 to 1200 X 1200 microns in retinal space) by changing the amplitude of the scanning mirrors.

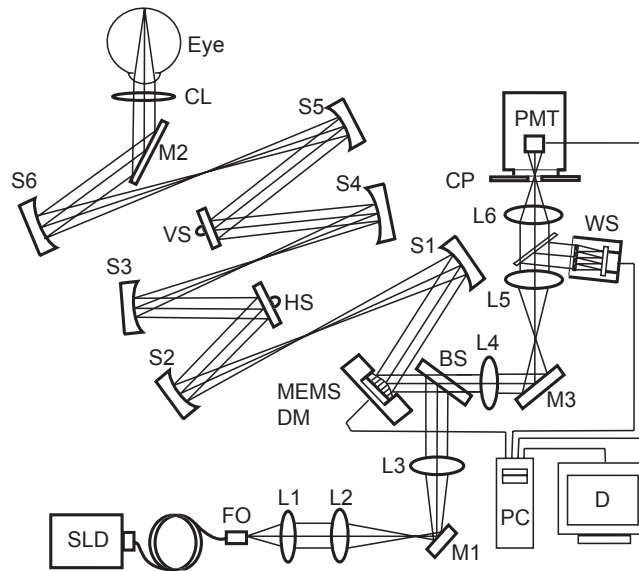


Fig.1. The MEMS DM based AOSLO. SLD, low coherent light source; FO, fiber output; PC, computer; D, display; BS, beam splitter; HS, horizontal scanner (16KHz), VS, vertical scanner (30, 60 Hz); CL, spherical and cylindrical lens for refractive correction; WS, wavefront sensor; CP, confocal pinhole; PMT, photomultiplier tube; M1~M3, flat mirrors; L1~L6, achromatic lenses; S1~S6, spherical mirrors.

The use of a compact MEMS DM has allowed us to reduce the entire size of the device to a footprint that is less than 50 X 50 cm. Furthermore the system is mounted on a rolling table which allows us to easily move it to the clinic. By comparison, the first-generation AOSLO, which uses a 37 channel discrete actuator DM (Xinetics Inc), occupies a space on an optical table that is 100 X 150 cm. Figure 3 shows a photograph of the system with specific components labeled.

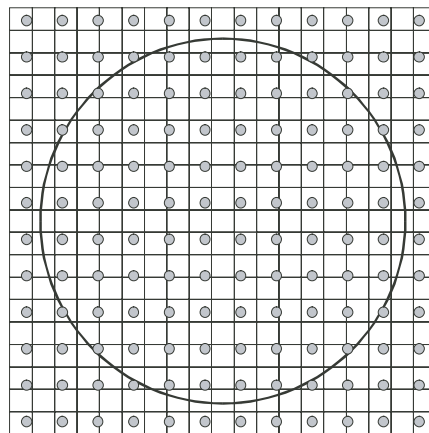


Figure 2: The figure shows the relative sizes and alignments of the pupil of the eye (black circle, 6 mm aperture) the lenslet array (square grid representing edges of the square-packed lenslet array) and the deformable mirror (gray circles representing actuator center locations). The eye, lenslet array and DM are all projected into a single plane, considering the relative magnification between them. Because the beam reflects off the DM obliquely, the actuators are effectively closer together in the horizontal direction than the vertical. The lenslet array samples the 6 mm pupil at 213 points and 80 actuators are used to drive the correction. To avoid edge effects, the aperture of the pupil at the collecting lens for the confocal pinhole is stopped down to 5.85 mm (projected into the eye-space), which is slightly smaller than the AO closed-loop aperture.

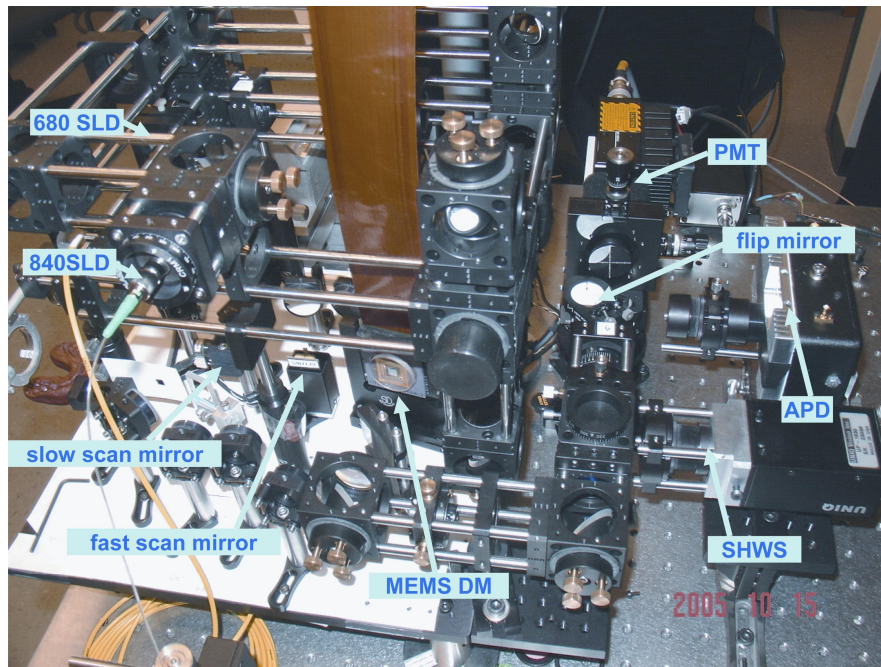


Figure 3: Photograph of the MEMS AOSLO. Most components are described in the text, except for the two separate input light ports, which are currently set up with 840 nm and 680 nm superluminescent diodes. There is also an option for either an avalanche photodiode (APD) or a photomultiplier tube (PMT) detector. Measurements in this paper were made with the 840-nm superluminescent diode and the PMT detector.

### 2.3. AOSLO Image Analysis

Video sequences are recorded directly to disk as uncompressed avi files. Images are analyzed and registered offline. The temporal nature of frame acquisition in an SLO, combined with the small field size, results in distortions of the retinal images which can be caused by even the smallest fixational eye movements. Custom software was developed to compensate for these eye movements and allow for accurate registration of multiple frames<sup>33</sup>. Registering multiple frames is an important step to improve the signal to noise of retinal images.

### 2.4. MEMS Mirror

The MEMS mirrors in the AOSLO is the  $\mu$ DMS-Multi<sup>TM</sup> from Boston Micromachines Corporation (Watertown, MA). The mirror consists of a single membrane supported by an underlying actuator array. Deflection of the mirror surface is via electrostatic attraction, and each actuator is individually addressable. Although the BMC mirror has a continuous membrane reflecting surface, it differs from a conventional membrane design. Cross-talk between actuators is minimized by constructing the actuator array with a double cantilever design. The mirror is described in detail in Bifano *et al*<sup>34</sup>. The specific mirror array is a 140 actuator design (12 X 12 with no corner actuators) over a 4.4 mm clear aperture. The actuator stroke is 3.5 microns.

The electrostatic actuation of the MEMS DM generates a monotonic, but non-linear deflection. Over the working range of the actuation, the response follows roughly a parabolic function. In addition, there is a membrane effect which causes the deflection of any one actuator to be dependent on the position of the neighboring actuators. The manufacturer provides voltage vs. deflection calibration curves for both a single actuator response and the complete array response. The second mode of operation generates the highest possible mirror deflections.

In order to operate the mirror in push-pull mode, the mirror is biased at its midpoint and voltage is either reduced or increased from the bias point.

## 2.5. AO Closed-Loop Operation

A modal approach is used to run the AO closed loop in the AOSLO. A 10<sup>th</sup> order Zernike polynomial is fitted to the wavefront slopes. The actuator deflections are then calculated directly from the best fit wavefront. Each actuator voltage is computed independently, assuming zero influence from its neighbors. Due to the broader influence function of each actuator, and the dependence of an actuator response on its neighboring actuator positions, we do not expect to achieve the desired shape in a single iteration. So, in order to obtain a good convergence, we use a gain less than one for each AO iteration and run the AO in a closed loop. Although we do not know the exact location of the actuator after each iteration, we do know that if the feedback loop operates fast enough, then each actuator will creep towards its optimal location. Since the eye's aberrations are dominated by static, rather than dynamic aberration, we can still achieve an acceptable correction with a relatively slow closed loop frequency of about 10 Hz. Nonetheless, correction of the dynamic aberrations is expected to yield a better correction<sup>25</sup>.

The magnification factors used in the system (fig 2) require that most of the diameter of the DM is used. Actuators whose centers fall outside the pupil are maintained at the bias voltage.

To avoid running out of mirror stroke, we relieve the stroke requirements on the mirror by minimizing 2<sup>nd</sup> order aberrations of the eye (defocus and astigmatism) with trial lenses prior to closing the loop. In practice, defocus and astigmatism are each corrected to less than 0.25 diopters of refractive error, which is the level of precision of available corrective trial lenses. After the best 2<sup>nd</sup> order correction, wavefront rms values of human eyes over 6 mm pupils range from 0.6 to 0.2 microns, depending on the individual.

In practice, we have obtained correction levels comparable, and often better, than those that obtained in our first generation AOSLO which uses a 37 element discrete actuator deformable mirror (Xinetics, Inc). Figure 4 shows the before and after AO correction RMS values for 10 normal healthy individuals. All but one subject were corrected to better than 0,1 microns RMS on average. RMS after AO was computed as the average RMS wave aberration from a series of AO iterations before and after convergence. It should be noted here that the RMS was computed from the Shack Hartmann wavefront measurement, which may not reflect exactly the residual aberrations. Before convergence, the values are accurate, but after convergence the values are likely dominated by noise.

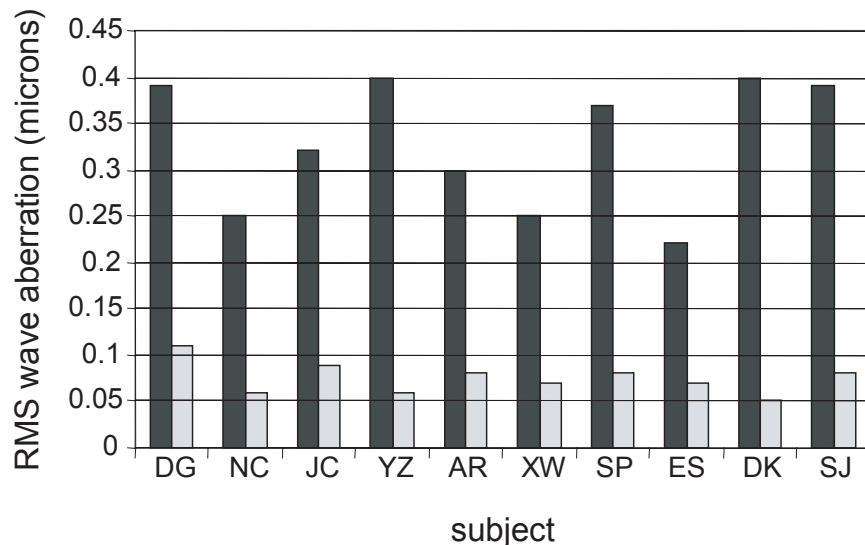


Figure 4: RMS wave aberrations of ten healthy subjects before and after AO correction with the MEMS deformable mirror.

In the first generation AOSLO, we used the deformable mirror to do fine focus adjustments in addition to correcting the aberrations. This has been shown to be a convenient, effective and economical way to move the focal plane through the thick retinal tissue<sup>35</sup>. We have not yet implemented the defocus control feature on the MEMS AOSLO.

### 3. RESULTS

Figure 5 shows retinal images before and after AO correction. The AO correction results in a triple benefit. First, the throughput is increased because the AO generates a smaller focused spot at the confocal pinhole passing more photons to the detector. Second the image has improved resolution because of the lateral resolution improvements of AO. Third, the image has higher contrast, due to improved rejection of light from out-of-focus layers. The last panel in the figure shows a co-added stack of 10 images of the same location. Every cone photoreceptor is resolved at this location. Figure 6 shows larger retinal patches from three different subjects. The images are comprised of a series of co-added frames that have been corrected for distortions due to eye movements and stitched together using Adobe Photoshop™ (San Jose, CA).

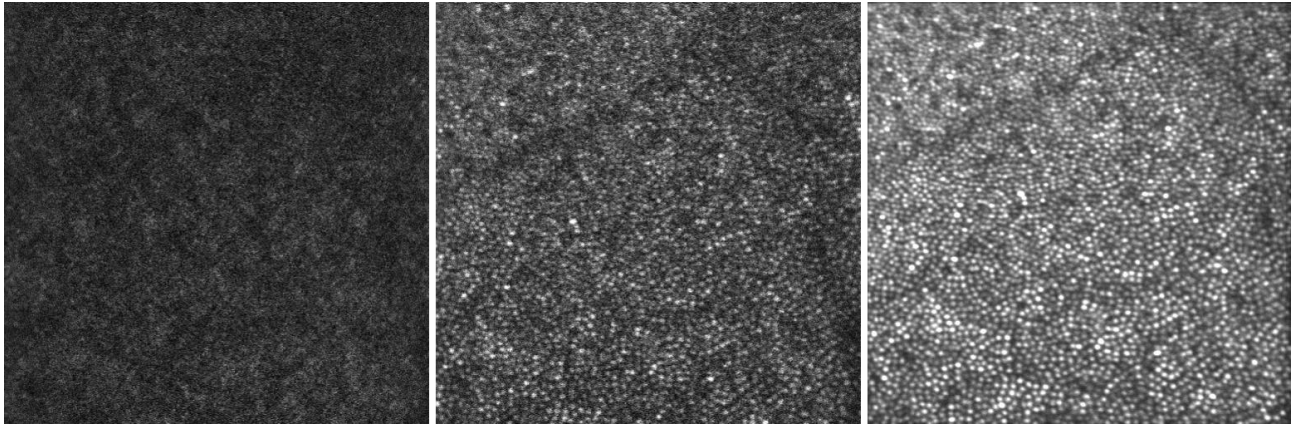


Figure 5: The left image is taken after best correction of defocus and astigmatism, but not high order aberrations. The second frame is a single frame taken after ASO correction. The third frame is a co-added set of 10 frames which have been corrected for distortions due to eye movements. Signal magnitude, resolution and contrast are improved after AO correction and virtually every cone is resolved in the registered frame.

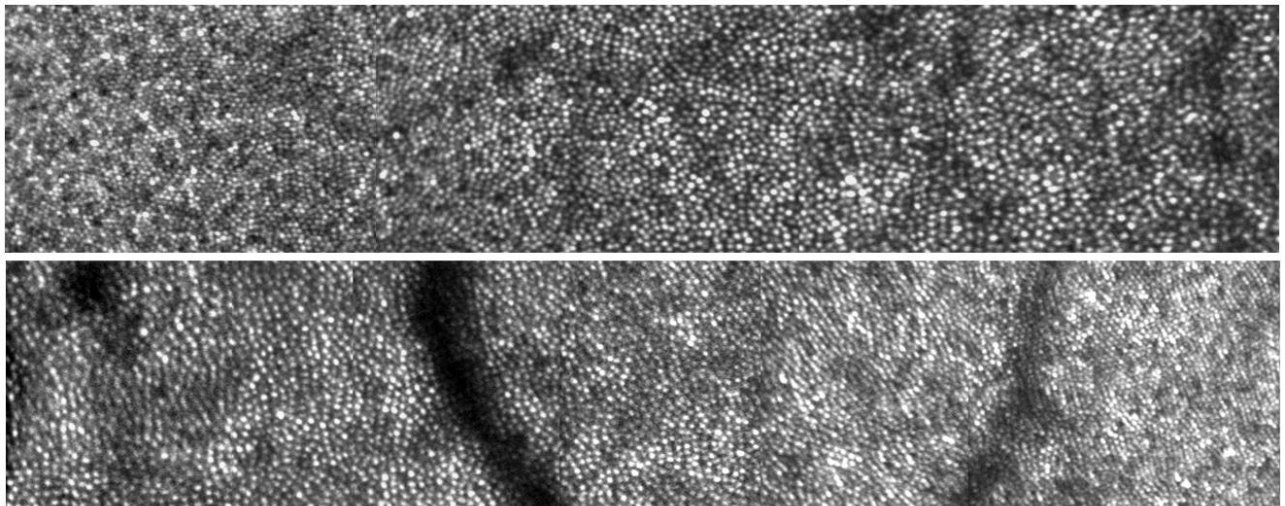


Figure 6: These two images show photoreceptors ranging in size as a function of eccentricity from the fovea from two different subjects. In the top image the span ranges from 0.6 to 3.72 degrees nasal to the fovea. In the lower image the span ranges from 1.11 to 4.23 degrees temporal to the fovea. The scale bar spans 0.5 degrees visual angle.

## 4. DISCUSSION AND CONCLUSIONS

The early results in this paper demonstrate the MEMS-based technology has matured to a level that compare with, if not improve upon, performance of discrete actuator DMs. Furthermore, the small size, the promise for increased stroke, and the potential for significantly lower cost make it likely that sometime in the near future discrete actuator DMs will be rendered obsolete for vision applications.

With future improvements, MEMS can potentially assume the role of other components in the system. For example, increased stroke will allow for use of the DM to move the focal plane through the thick retinal tissue. It may also obviate the need for lenses to compensate for the 2<sup>nd</sup> order aberrations of defocus and astigmatism. If the increased stroke is combined with increased speed, it may facilitate some tip-tilt adjustment to stabilize the retina image or to pan the raster across different regions of the retina. The best scenario, and one that would greatly reduce the price complexity and cost of an AOSLO, would be to implement a MEMS device that could simultaneously correct all the aberrations, adjust the focal plane within the retina, pan the raster scan to different regions of the retina, and perform the raster scan (which would require extremely fast tip/tilt control).

## ACKNOWLEDGEMENTS

This work was funded by the National Institutes of Health Bioengineering Research Partnership Grant EY014375 and the National Science Foundation Science and Technology Center for Adaptive Optics, managed by the University of California at Santa Cruz under cooperative agreement #AST-9876783.

## REFERENCES

1. J. Liang, D. R. Williams, and D. Miller. "Supernormal vision and high-resolution retinal imaging through adaptive optics," *J.Opt.Soc.Am.A* **14**, 2884-2892. 1997.
2. A. Roorda and D. R. Williams. "The arrangement of the three cone classes in the living human eye," *Nature* **397**, 520-522. 1999.
3. A. Roorda and D. R. Williams. "Optical fiber properties of individual human cones," *J.Vision* **2**, 404-412. 2002.
4. A. Pallikaris, D. R. Williams, and H. Hofer. "The reflectance of single cones in the living human eye," *Invest Ophthalmol.Vis.Sci.* **44**, 4580-4592. 2003.
5. H. Hofer, B. Singer, and D. R. Williams. "Different sensations from cones with the same pigment," *J.Vision* **5**, 444-454. 2005.
6. H. Hofer, J. Carroll, J. Neitz, M. Neitz, and D. R. Williams. "Organization of the human trichromatic cone mosaic," *J.Neurosci.* **25**, 9669-9679. 2005.
7. J. Carroll, M. Neitz, H. Hofer, J. Neitz, and D. R. Williams. "Functional photoreceptor loss revealed with adaptive optics: an alternate cause of color blindness," *Proc.Natl.Acad.Sci.U.S.A* **101**, 8461-8466. 2004.
8. A. Roorda, F. Romero-Borja, W. J. Donnelly, H. Queener, T. J. Hebert, and M. C. W. Campbell. "Adaptive optics scanning laser ophthalmoscopy," *Optics Express* **10**, 405-412. 2002.
9. S. B. Stevenson and A. Roorda, "Correcting for miniature eye movements in high resolution scanning laser ophthalmoscopy," in *Ophthalmic Technologies XI*, F. Manns, P. Soderberg, and A. Ho, eds. Proceedings of SPIE Vol. **5688A**, 145-151. (SPIE, Bellingham, WA, 2005).
10. J. A. Martin and A. Roorda. "Direct and non-invasive assessment of parafoveal capillary leukocyte velocity," *Ophthalmology* **112**, in press. 2005.
11. L. Zhu, P.-C. Sun, D. U. Bartsch, W. R. Freeman, and Y. Fainman. "Adaptive control of a micromachined continuous-membrane deformable mirror for aberration compensation," *Appl.Opt.* **38**, 168-176. 1999.
12. E. J. Fernandez and P. Artal. "Membrane deformable mirror for adaptive optics: performance limits in visual optics," *Optics Express* **11**, 1056-1069. 2003.
13. D. Horsley, H. Park, S. P. Laut, and J. S. Werner, "Characterization for vision science applications of a birmorph deformable mirror using phase-shifting interferometry," in *Ophthalmic Technologies XV*, F. Manns, P. Soderberg, A. Ho, B. E. Stuck, and M. Belken, eds. Proceedings of SPIE Vol. **5688**, 133-144. (SPIE, Bellingham, WA, 2005).

14. E. Dalimier and C. Dainty. "Comparative analysis of deformable mirrors for ocular adaptive optics," *Optics Express* **13**, 4275-4285. 2005.
15. L. N. Thibos and A. Bradley. "Use of liquid-crystal adaptive-optics to alter the refractive state of the eye," *Optom.Vis.Sci.* **74**, 581-587. 1999.
16. F. Vargas-Martin, P. M. Prieto, and P. Artal. "Correction of the aberrations in the human eye with a liquid-crystal spatial light modulator: limits to performance," *J.Opt.Soc.Am.A Opt.Image Sci.Vis.* **15**, 2552-2562. 1998.
17. D. T. Miller, L. N. Thibos, and X. Hong. "Requirements for segmented correctors for diffraction-limited performance in the human eye," *Optics Express* **13**, 275-289. 2005.
18. A. Awwal, B. Bauman, D. Gavel, S. Olivier, S. Jones, D. Silva, J. L. Hardy, T. Barnes, and J. S. Werner, "Characterization and operation of a liquid crystal adaptive optics phoropter," in *Astronomical Adaptive Optics Systems and Applications*, R. K. Tyson and Lloyd-Hart M., eds. Proceedings of SPIE Vol. **5169**, 104-122. (SPIE, Bellingham, WA, 2003).
19. P. M. Prieto, E. J. Fernandez, Manzanera S., and P. Artal. "Adaptive optics with a programmable phase modulator: applications in the human eye," *Optics Express* **12**, 4059-4071. 2004.
20. G. J. van Blokland and D. van Norren. "Intensity and polarization of light reflected at small angles from the human fovea," *Vision Res.* **26**, 485-494. 1986.
21. G. J. van Blokland and S. C. Verhelst. "Corneal polarization in the living human eye explained with a biaxial model," *J.Opt.Soc.Am.A* **4**, 82-90. 1987.
22. N Doble and D. T. Miller, "Wavefront Correctors for Vision Science," in *Adaptive Optics for Vision Science: Principles, Practice, Design and Applications*, J. Porter, A. Awwal, J. Lin, H. Queener, and K. Thorn, eds. (Wiley & Sons) **in press**.
23. J. Porter, A. Guirao, I. G. Cox, and D. R. Williams. "Monochromatic aberrations of the human eye in a large population," *J.Opt.Soc.Am.A* **18**, 1793-1803. 2001.
24. L. N. Thibos, X. Hong, A. Bradley, and X. Cheng. "Statistical variation of aberration structure and image quality in a normal population of healthy eyes," *J.Opt.Soc.Am.A* **19**, 2329-2348. 2002.
25. H. Hofer, P. Artal, J. L. Aragon, and D. R. Williams. "Dynamics of the eye's wave aberration," *J.Opt.Soc.Am.A* **18**, 497-506. 2001.
26. N Doble, G Yoon, P Bierden, L. Chen, S Olivier, and D. R. Williams. "Use of a microelectromechanical mirror for adaptive optics in the human eye," *Optics Letters* **27**, 1537-1539. 2002.
27. R. H. Webb, G. W. Hughes, and F. C. Delori. "Confocal scanning laser ophthalmoscope," *Appl.Opt.* **26**, 1492-1499. 1987.
28. T. Wilson and C. J. R. Sheppard. "Theory And Practice of Scanning Optical Microscopy," Academic Press, (London, 1984).
29. M. Minsky. "Memoir on Inventing the Confocal Scanning Laser Microscope," *Scanning* **10**, 128-138. 1988.
30. T. Wilson, "The role of the pinhole in confocal imaging systems," in *The Handbook of Biological Confocal Microscopy*, J. B. Pawley, ed. pp. 99-113. (Plenum Press, New York, 1990)
31. J. Liang and D. R. Williams. "Aberrations and retinal image quality of the normal human eye," *J.Opt.Soc.Am.A* **14**, 2873-2883. 1997.
32. A. Roorda and Y. Zhang. "Mechanism for cone reflectance revealed with low coherence AOSLO imaging," *Invest.Ophthalmol.Vis.Sci.* **46**, E-Abstract 2433. 2005.
33. C. R. Vogel, D. Arathorn, A. Roorda, and A. Parker. "Retinal motion estimation and image dewarping in adaptive optics scanning laser ophthalmoscopy," *Optics Express* **in press**
34. T. G. Bifano, J. A. Perreault, P. A. Bierden, and C. E Dimas, "Micromachined deformable mirrors for adaptive optics," in *High Resolution Wavefront Control: Methods, Devices, and Applications IV*, J. D. Gonglewski, M. A. Vorontsov, M. T. Gruneisen, S. R. Restaino, and R. K. Tyson, eds. Proceedings of SPIE Vol. **4825**, 10-13. (SPIE, Bellingham, WA, 2002).
35. F. Romero-Borja, K. Venkateswaran, A. Roorda, and T. J. Hebert. "Optical slicing of human retinal tissue *in vivo* with the adaptive optics scanning laser ophthalmoscope," *Appl.Opt.* **44**, 4032-4040. 2005.